*European Journal of Soil Science*

WILEY

RESEARCH ARTICLE OPEN ACCESS

# Thermodynamics of Organic Acid Sorption to Goethite

Alexander Konrad[1] | Ines Mulder[1,2] | Diana Hofmann[3] | Friederike Lang[4] | Kenton P. Stutz[4] | Jan Siemens[1]

[1]Justus-Liebig-University Giessen, Institute of Soil Science and Soil Conservation, Giessen, Germany | [2]Department Soil Sciences and Soil Resources, Institute of Geography, Ruhr University Bochum, Bochum, Germany | [3]Forschungszentrum Jülich, Institute of Bio- and Geosciences, Agrosphere (IBG-3), Jülich, Germany | [4]Albert-Ludwigs-Universität Freiburg, Institute of Forest Sciences, Chair of Soil Ecology, Freiburg im Breisgau, Germany

**Correspondence:** Alexander Konrad (alexander.konrad@umwelt.uni-giessen.de)

**Received:** 30 May 2025 | **Revised:** 28 November 2025 | **Accepted:** 29 December 2025

**Keywords:** carbon cycle | carbon sequestration | isothermal titration calorimetry | low molecular weight organic compound | mineral-associated organic matter | soil

## ABSTRACT

Adsorption to minerals is a key mechanism in stabilizing organic carbon in soils. We used isothermal titration calorimetry (ITC) to quantify the thermodynamics of binding of citric acid, oxalic acid, and salicylic acid to four goethites with different specific surface areas (SSA, 14–120 $m^2\ g^{-1}$). Thermodynamic parameters could be determined for sorption of citric and salicylic acids, while flocculation of particles prevented their quantification for sorption of oxalic acid. For citric acid adsorption, $\Delta H$ shifted from $-23.5 \pm 0.57$ to $-27.0 \pm 0.47$ kJ $mol^{-1}$ and $\Delta S$ from $-8.8 \pm 1.54$ to $-29.9 \pm 0.13$ J $mol^{-1}\ K^{-1}$ with increasing SSA and broader (110) diffraction peaks of goethite, thus reducing $\Delta G$ from $-20.7 \pm 0.02$ to $-18.0 \pm 0.03$ kJ $mol^{-1}$. Salicylic acid adsorption was more exothermic ($\Delta H$ $-40.53 \pm 1.93$ kJ $mol^{-1}$) and accompanied by a larger loss of entropy ($\Delta S$ $-65.1 \pm 1.91$ J $mol^{-1}\ K^{-1}$), possibly due to chelation of its ortho hydroxyl and carboxyl groups to single iron atoms on the mineral surface. These results demonstrate that ITC can decipher adsorption thermodynamics of organic ligands to mineral surfaces, but ligand-induced flocculation can render the interpretation of results difficult. Crystallite size and lattice defects of adsorbent minerals influence the thermodynamics of sorption by determining the conformation of organic molecules sorbed to goethite surfaces.

## 1 | Introduction

The fate of organic carbon (OC) in soils is extensively researched as soil represents the largest terrestrial C sink (Georgiou et al. 2022). Sorption to minerals slows down OC mineralization, as demonstrated by age distributions of OC across soil depths and fractions (Saidy et al. 2015; Schrumpf et al. 2013; Spielvogel et al. 2008). Besides clay minerals, iron (oxyhydr-)oxides such as goethite are some of the most common pedogenic minerals (Cornell and Schwertmann 2003; Guo and Barnard 2013). Goethite commonly forms needle-shaped crystals and exhibits exceptional sorption capacities for anions or zwitterionic solutes due to the net positive surface charges in acidic and neutral soils (Bramble et al. 2024; Feng et al. 2013; Gao et al. 2018; Georgiou et al. 2022; Saidy et al. 2012). In soils, the introduction of impurities and variable boundary conditions of mineral formation (Schwertmann et al. 1985) cause crystallographic defects, like line defects (dislocation) (Taitel-Goldman et al. 2004), point defects (vacancies) (Madsen et al. 2009), and substitutional defects (Goodman and Lewis 1981). Generally the number of defects and the specific surface area (SSA) increase with decreasing size of goethite crystallites (Schwertmann et al. 1985; Taitel-Goldman et al. 2004). Defect density of goethite has been shown to play an important role for the adsorption of arsenic moieties of organometallic complexes (Hou et al. 2022), phosphate (Strauss et al. 1997), and OC (Kaiser and Guggenberger 2003, 2007; Mikutta et al. 2004). Despite the relevance of sorption of organic molecules on oxyhydroxide mineral surfaces to the stabilization of OC, their thermodynamics, namely sorption

**Highlights**

- First complete assessment of $\Delta H$, $\Delta S$, and $\Delta G$ of sorption of organic acids to goethites.
- Flocculation of mineral particles must be prevented to obtain meaningful ITC data.
- Goethite particle size & crystallinity modulate the thermodynamics of citric acid sorption.
- Sorption of organic acids to goethite does not present an energetic barrier for their mineralization.

enthalpy ($\Delta H$), Gibbs free energy ($\Delta G$), and entropy ($\Delta S$), have not been quantified to date.

Isothermal titration calorimetry (ITC) is a method able to quantify the thermodynamics of binding-reactions within a single experiment and is regarded as gold standard for studying the thermodynamics of molecular interactions in solution (Bastos et al. 2023). In an ITC experiment, known amounts of sorbate are sequentially titrated into a constantly stirred reaction chamber filled with known amounts of sorbent and the heat released or consumed during the binding reaction is measured (Freire et al. 1990; Wiseman et al. 1989). While ITC is routinely used to investigate the binding of ligands to macromolecules, the technique has rarely been applied for the study of adsorption of ligands to solid materials (Joshi et al. 2004; Prozeller et al. 2019). The usage of suspended nanoparticles as sorbent increases the complexity of interactions during the ITC experiment, especially by potential flocculation of particles (Jódar-Reyes et al. 2001). Nonetheless, this technique has been used to study the sorption of orthophosphate to kaolinite (Penn and Warren 2009), soil slurries (Penn and Zhang 2010), gibbsite (Hong et al. 2020), and clay-sized mineral mixtures extracted from soils (Hong et al. 2021) as well as uranium on goethite (Kumar et al. 2022). However, only the studies conducted with gibbsite and clay mineral mixtures obtained ITC data suitable to calculate the desired thermodynamic characteristics (Hong et al. 2020, 2021).

The aim of this study was to explore the potential and limitations of ITC to elucidate the thermodynamics of sorption of small organic acids to goethite. Oxalic acid, citric acid, and salicylic acid were chosen as organic model ligands because of their ubiquity in soil and strong binding affinities to goethite (Jones and Edwards 1998; Yeasmin et al. 2014). Four goethite minerals of different crystallinity, specific surface area (SSA), and density of surface defects were investigated. Sorption was studied at a slightly acidic pH of 5.5. We hypothesized, that (1) sorption of oxalic- and citric acid yield similar changes in enthalpy $\Delta H$ and Gibb's free energy $\Delta G$ at pH 5.5 as both ligands contain two deprotonated carboxyl groups at that pH, and (2) $\Delta H$ and $\Delta G$ of ligand adsorption to minerals increase with increasing surface area and increasing number of defects of minerals.

## 2 | Materials and Methods

All chemicals were purchased from Sigma Aldrich (Darmstadt, Germany), with purities >99%. Ultra-pure water was sourced from a Purelab Flex 2 Water Purification System (Veolia Water Solutions and Technologies, Buchinghamshire, United Kingdom).

### 2.1 | Goethite Synthesis and Characterization

Commercially available goethite BAYFERROX 920Z (LANXESS Deutschland GmbH, Cologne, Germany) and three self-synthesized goethite minerals were used for this study. Two iron hydroxides were synthesized using 10 M NaOH titrated into a constantly stirred, freshly prepared 0.5 M $FeCl_3$ solution up to pH 12 (Dultz et al. 2019). To create hydroxides with different specific surface areas, the suspensions were stored for 68 days at 4°C and 8°C, respectively, before adjustment to pH 6 with 0.2 M HCl. The third goethite was synthesized by aeration of an $NaHCO_3$-buffered 0.05 M $FeCl_2$ solution with compressed air injected through perforated polyethylene tubes (Goodman and Lewis 1981; Fischer et al. 1998). Mineral suspensions were filled into Spectra/Por 2 dialysis membranes with a molecular weight cut-off of 12–14 kDa and dialyzed against deionized water until the conductivity of the suspensions dropped below 5 $\mu S\ cm^{-1}$. All suspensions were afterwards freeze-dried and ground using a mortar and pestle.

Mineral purity was confirmed via X-ray powder diffraction using an Empyrean 3 X-ray diffractometer (Malvern-PANanalytical B.V, Worcestershire, Great Britain) equipped with a copper source. Specific surface areas, pore volume, and pore size distribution of mesopores were investigated via nitrogen sorption at 77 K after drying for 18 h at 65°C (single measurements; instrument reproducibility ±1%) using a Quantachrome Quadrasorb evo (Anton Paar Germany GmbH, Ostfildern-Scharnhausen, Germany). The morphology of goethite was studied with a scanning electron microscope (SEM) GeminiSEM 560 (Carl Zeiss Microscopy Deutschland GmbH, Oberkochen, Germany) after mounting on sample holders with carbon tabs.

### 2.2 | Isothermal Titration Calorimetry

Experimental setups for all investigated mineral phases and organic acid combinations followed the same general procedure: Heat production or consumption during adsorption of carboxylic acids as ligands on mineral surfaces was measured with a dynamically calibrated thermal activity monitor 3 (TAM 3, TA Instruments Inc., Newcastle, Delaware, USA) equipped with a 4 mL nanocalorimeter. The reference ampoule of the calorimeter was filled with suspensions of the same mineral and exchanged weekly to prevent sedimentation. To minimize differences in heat capacity between the measurement and reference cells, the reference unit contained an equivalent dummy setup including the shaft and propeller. The calorimeter was dynamically calibrated after each suspension change to account for potential differences in suspension heat capacity. Mineral suspensions and ligand solutions of varying concentrations in 0.01 M KCl background electrolyte were adjusted to pH 5.5 ± 0.01 with HCl and KOH to mitigate the heat signal of the acid–base neutralization during titration. Sorbate solutions were filtered through <220 nm polyether sulfone syringe filters in a sterile environment. The calorimeter syringe system was rinsed several times, first with 0.1 M HCl to remove potential goethite, followed ethanol to reduce the

risk of microbial processing of the organic sorbates. Sorbents and sterile-filtered sorbates were degassed under vacuum for 30 min, followed by 5 min in an ultrasonic bath at room temperature. The titration unit was assembled under sterile conditions afterwards. The system was equilibrated prior to titration to reach thermal stability (standard deviation < 50 nW, slope < 50 nW $h^{-1}$). After temperature equilibration, experiments during method development consisted of 20–40 titrations at 25°C with volumes from 0.5 to 3 μL, dosing-speeds of 0.1–1 μL $s^{-1}$ and titration intervals between 8 and 30 min into mineral suspensions ranging from 5 and 40 g $L^{-1}$. Potential organic acid-induced mineral dissolution during titration experiments was investigated by analyzing dissolved iron in the suspensions after ITC experiments. To this end, suspensions were centrifuged at 17,000*g* for 60 min and the supernatant analyzed using inductively coupled plasma optical emission spectroscopy (ICP-OES) (Agilent 720, Agilent Technologies Inc., Santa Clara, USA). Subsequently, blank measurements were performed by repeating ITC experiments with 0.01 M KCl solutions (likewise adjusted to pH 5.5) instead of mineral suspensions to subtract the heat of dilution from ligand titration into the mineral suspensions.

### 2.3 | Data Analysis

Experimental raw data (e.g., time evolved, timing of the consecutive injections, heat flow) were exported from the calorimeter using TAM Assistant 3.0 (TA Instruments Inc., Newcastle, Delaware, USA). Baseline correction was performed with Origin Pro 2024b (OriginLab Corporation, Northampton, MA, USA), using the integrated asymmetric least square smoothing function (Eilers and Boelens 2005). Baseline-corrected data were subsequently exported to NanoAnalyze 4.0.2 (TA Instruments Inc., Newcastle, Delaware, USA), integrated for heat flows, and corrected for blank titrations. An exemplary workflow for raw data processing is shown in Supporting Information S1.

The adsorption thermodynamics was modeled using the independent, one-site binding model integrated into the NanoAnalyze software based on the Wiseman isotherm (Wiseman et al. 1989). The Wiseman isotherm was developed and is typically used for analyzing the binding of ligands to biological macromolecules. This model assumes that (1) all binding sites are considered identical with the same affinity for the ligand, (2) the binding of a ligand to one site does not affect the binding at another site, and (3) that the number of binding sites for ligands per macromolecule equals 1. Application of this isotherm to the binding of ligands to a mineral surface requires a careful consideration of dimensions of the variables that are used as input for the modeling of the binding reaction. The one-site binding model typically used to describe ligand-macromolecule interactions expresses the concentrations of ligands, macromolecular sorbent and ligand-macromolecular complexes in the dimension [mol $L^{-1}$]. For describing the binding of ligands to mineral surfaces, a former study therefore determined the number of reactive binding sites on the surface of their gibbsite minerals in separate potentiometric titration experiments (Hong et al. 2020) to derive the concentration of gibbsite binding sites in [mol $L^{-1}$] for the interpretation of their ITC experiments. In order to derive all sorption and thermodynamic parameters in a single ITC experiment, we decided to use instead the surface area of the minerals as direct input and thus express the concentration of the sorbent as [$m^2 L^{-1}$]. This adjustment will not affect the value of $\Delta H$ that is determined in the titration experiment, since ΔH is derived directly from changes of the measured heat flow. Similarly, this uncommon dimension of the sorbent concentration will not affect the estimation of the association constant $K_a$ from the titration experiment, because $K_a$ is considered in the Wiseman equation via the parameter *r*, in which $K_a$ is combined with total mineral surface concentration, so that the units of $K_a$ and sorbent concentration cancel out (Wiseman et al. 1989, 1). The parameter *r* and hence $K_a$ are derived from the slope of the sigmoidal binding curve at its inflection point. However, when applying the Wiseman model for the interpreting the titration experiments with the dimension [$m^2 L^{-1}$] for the sorbent concentration, we have to consider that the dimension of the *x*-axis of the binding curve in our case is not dimensionless, but in the unit [mol $m^{-2}$]. If the assumption of one binding site per unit of sorbent is met, then the inflection point of the sigmoidal binding curve is exactly at a ratio of 1 on the *x*-axis, which describes the binding stoichiometry *n*. Hence, when plotting the *x*-axis of the binding curve in the dimension [mol ligand $m^{-2}$ mineral surface area], the parameter *n* directly indicates the number of sorption sites per $m^2$ surface area of the mineral. To test the feasibility of our approach, we repeated the estimation of thermodynamic parameters and $K_a$ after transforming the sorbent concentration from the unit [$m^2 L^{-1}$] into [mol binding sites $L^{-1}$] by multiplying the parameter *n* retrieved from the one site binding model with the surface area concentration [$m^2 L^{-1}$] in our suspension. Using this value as input for *M* (now in mol binding sites $L^{-1}$ mineral suspension) yielded a parameter *n* of 1 (Figure S2). The estimated thermodynamic parameters of adsorption, including $K_a$ remained unchanged, confirming the applicability of our approach.

The Gibbs free energy of adsorption $\Delta G$ and the entropy change ΔS of the sorption reaction can be derived from general thermodynamic relationships. The Gibbs free energy of adsorption $\Delta G$ [J $mol^{-1}$] is related to the equilibrium association constant $K_a$ (Equation 1):

$$\Delta G = -RT \ln(K_a) \quad (1)$$

where *R* is the gas constant [J $K^{-1}$ $mol^{-1}$] and *T* the temperature [K]. Adsorption $\Delta G$ can be separated into enthalpic ($\Delta H$ [J $mol^{-1}$]), as well as entropic ($\Delta S$ [J $mol^{-1}$ $K^{-1}$]) contributions via equation (Equation 2):

$$\Delta G = \Delta H - T\Delta S \quad (2)$$

Successful ITC experiments were repeated in triplicates, with the thermodynamics of each experimental replicate modeled separately. Inverse variance-weighted means were computed from values $x_i$ with standard errors $\sigma_i$ for modeled thermodynamic parameters with standard errors, e.g., $\Delta H$ and *n* (Equation 3):

$$\bar{x} = \frac{\sum_{i=1}^{n} \frac{x_i}{\sigma_i^2}}{\sum_{i=1}^{n} \frac{1}{\sigma_i^2}} \quad (3)$$

The standard errors of the weighted means $\sigma_{\bar{x}}$ are given by (Equation 4):

$$\sigma_{\bar{x}} = \sqrt{\frac{1}{\sum_i^n \frac{1}{\sigma_i^2}}} \quad (4)$$

Means of modeled parameters without standard errors, e.g., $\Delta G$, $\Delta S$ and $K_a$ were calculated as arithmetic means.

## 3 | Results and Discussion

### 3.1 | Characteristics of Minerals

The SSA of minerals ranged from 13.8 $m^2g^{-1}$ for commercial BAYFERROX goethite to 119.6 $m^2g^{-1}$ for goethite synthesized using compressed air (Figure 1). For convenience, we refer to these minerals as Goe-14 (13.8 $m^2g^{-1}$), Goe-93 (92.6 $m^2g^{-1}$), Goe-112 (111.9 $m^2g^{-1}$) and Goe-120 (119.6 $m^2g^{-1}$). Scanning electron microscope (SEM) images showed comparably large elongated rhombic shapes with clear crystal faces for Goe-14, clear needle-like shapes for Goe-93 and Goe-112, and finer grain structures for Goe-120 (Figure 1). Powder X-ray diffraction (XRD) spectra confirmed that all minerals were pure goethite, with XRD peaks broadening with increasing SSA (Figure 1). The full width at half maximum (FWHM) of each 110 peak ($FWHM_{110}$) after baseline correction increased with increasing SSA, thus indicating a decreasing crystallinity with increasing SSA (Supporting Information S3 and Table 1). This relationship corresponded with the crystal morphology observed with SEM, as reported earlier (Echigo et al. 2012).

### 3.2 | Preliminary Experiments to Avoid Flocculation and Dispersion

Ligand-induced flocculation and dispersion emerged as the main challenge in obtaining usable data during our ITC experiments. We identified four distinct patterns of flocculation (Figure 2). We could not achieve a stable suspension with the most crystalline goethite Goe-14. Within minutes of starting the agitator, colloids flocculated and settled at the bottom of the measuring ampoule (Figure 2a). Despite this sedimentation, the ITC experiment with citric acid and flocculated goethite revealed small exothermic heat spikes followed by endothermic spikes with amplitudes

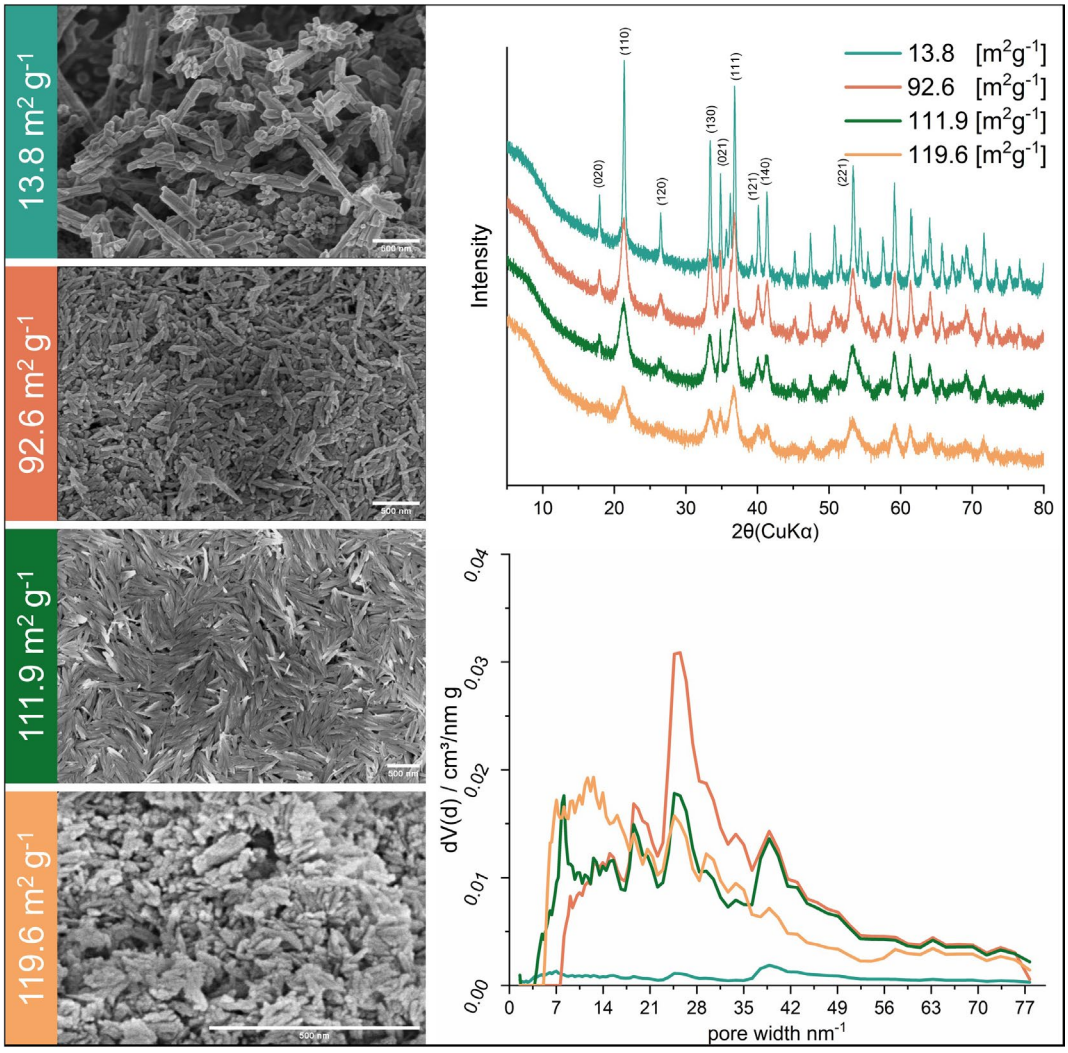


**FIGURE 1** | Scanning electron microscopy recordings of synthesized goethite with specific surface areas from 13.8 $m^2g^{-1}$ (top left), up to 119.6 $m^2g^{-1}$ (bottom left), with powder X-ray diffractograms and pore size distribution of the four goethite samples (right).

**TABLE 1** | Thermodynamics of adsorption of citric acid to goethite of specific surface areas (SSA) of 92.6 to 119.6 $m^2 g^{-1}$ and salicylic acid to goethite of SSA of 119.6 $m^2 g^{-1}$.

| | | Citric acid | | Salicylic acid |
|---|---|---|---|---|
| SSA [$m^2 g^{-1}$] | 92.6 | 111.9 | 119.6 | 119.6 |
| $FWHM_{110}$ [2θ] | 0.799 | 1.013 | 1.128 | 1.128 |
| $K_a$ [$mol^{-1}$] | 4348 ± 37 | 2703 ± 47 | 1449 ± 28 | 6667 ± 41 |
| $n$ [μmol $m^{-2}$] | 1.71 ± 0.1 | 2.79 ± 0.1 | 2.77 ± 0.0 | 0.20 ± 0.0 |
| $\Delta H$ [kJ $mol^{-1}$] | −23.5 ± 0.6 | −24.0 ± 0.7 | −27.0 ± 0.5 | −40.53 ± 1.9 |
| $\Delta G$ [kJ $mol^{-1}$] | −20.7 ± 0.0 | −19.6 ± 0.0 | −18.0 ± 0.0 | −21.7 ± 0.1 |
| $\Delta S$ [J $mol^{-1} K^{-1}$] | −8.8 ± 1.5 | −15.0 ± 0.4 | −29.9 ± 0.1 | −65.1 ± 1.9 |
| $-T\Delta S$ [kJ $mol^{-1}$] | 2.6 ± 0.6 | 4.1 ± 0.4 | 8.9 ± 0.0 | 19.4 ± 0.6 |

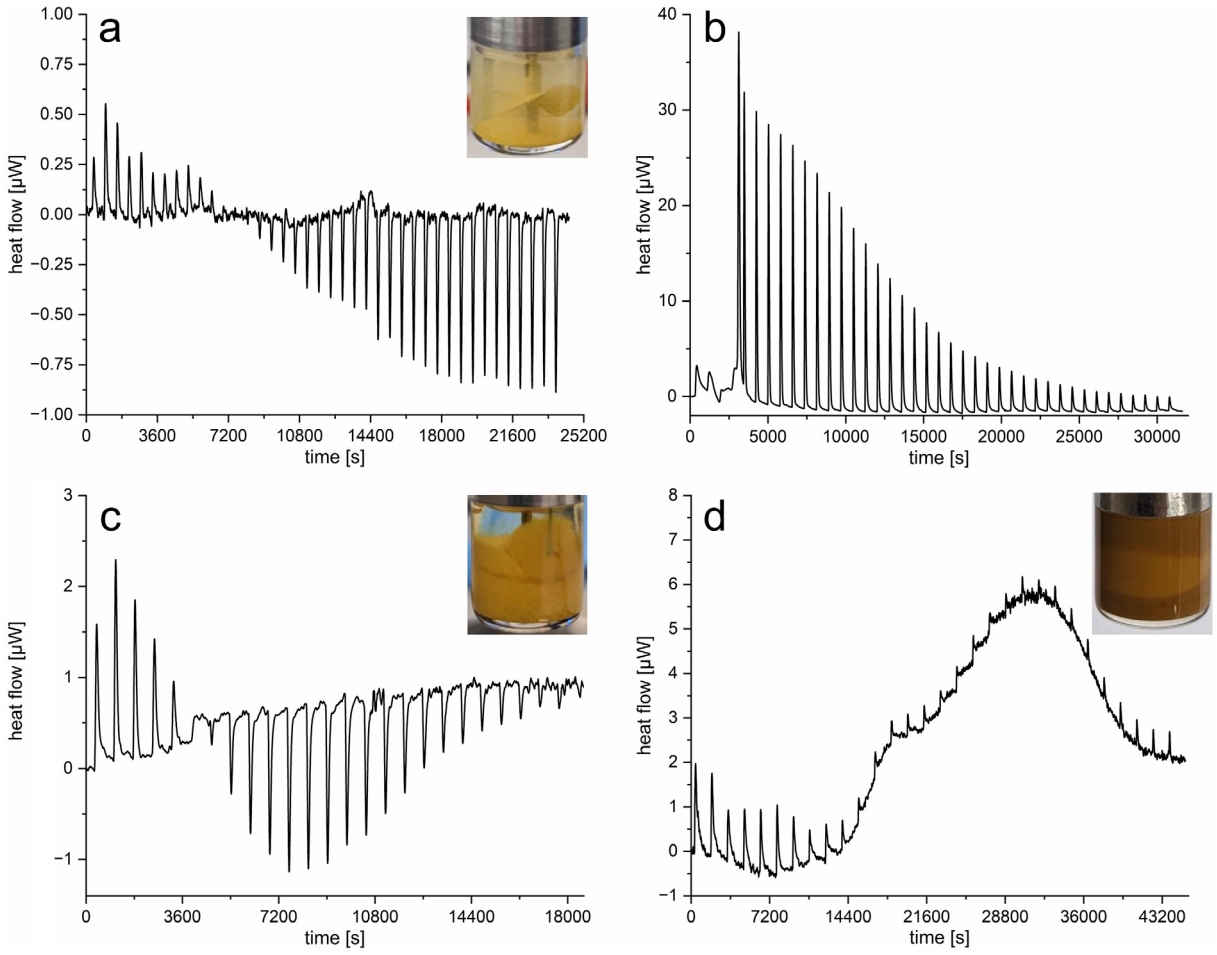


**FIGURE 2** | Flocculation observed during method development in isothermal titration calorimetry experiments with no baseline correction applied. (a) Goe-14 with citric acid showed flocculation and sedimentation, accompanied by low exothermic heat signals, followed by low endothermic heat flow spikes. (b) High dosage speeds of citric acid into Goe-112 lead to noisy heat spikes during the initial injections of sorbate solution of the experiment. (c) Thermograms of oxalic acid adsorption to Goe-93 with exothermic signals followed by endothermic signals and flocculation of the mineral phase. (d) Salicylic acid adsorption to Goe-112 with strong baseline shifts and two-toned suspension after the experiment.

smaller than 1 μW. Since no dissolved iron was found in the suspension after the experiment, we exclude dissolution of goethite by citric acid as a reason for the heat production and consumption. Thus, we conclude that only flocculation and dispersion dominated the heat flow in this experiment.

A second flocculation phenomenon occurred when the sorbate injection rate exceeded 0.1 μL $s^{-1}$. Above this dosage speed, sorbates did not mix properly with the suspension during the initial titrations. Instead, noisy and time-delayed exothermic signals were generated (Figure 2b).

The third flocculation phenomenon was observed when oxalic acid was injected into any goethite suspension. Oxalate caused flocculation and immobilization of colloids around the injection cannula (Figure 2c), which induced partial sedimentation and a clear supernatant at the end of the sorption experiment even while the agitator was still running. Since no dissolved iron was found in the suspension, bridging of goethite particles by monodentate binding of oxalic acid molecules to different mineral surfaces was most likely the driver of flocculation. Indeed, FTIR measurements showed that goethite-adsorbed oxalic acid formed monodentate structures with the ligand's two carboxylic acid functional groups being bound to different hydroxyl groups on minerals surfaces (Yeasmin et al. 2014). Therefore, the contribution of flocculation and ligand-exchange to heat flow cannot be disentangled.

Lastly, sequential titration of salicylic acid to Goe-93 and Goe-112 led to reproducible baseline shifts (Figure 2d). After disassembling the reaction ampoule, we observed that the suspension surrounding the agitator changed color (Figure 2d). The calorimeter's agitator operates at constant power, but a change in the suspension's viscosity during titration would have caused friction-induced heat to enter the calorimeter shifting the baseline, with observations of high viscosity in flocculated aqueous goethite suspensions and water-like viscosity in dispersed suspensions support this theory (Blakey and James 2003). While software can correct these baseline shifts, the two-toned suspension observed after the experiment raises concerns about adequate mixing of minerals and sorbates, and therefore the validity of the obtained thermodynamic parameters.

We tried to prevent flocculation phenomena by enhancing the intermixing of the suspension through agitator modifications. The shaft of the standard agitator, the 18 carat golden propeller, was shortened to fit two stacked agitators within the suspension of the measurement ampoule. In other experimental trials, 3D-printed helical polypropylene agitators were placed into reference and measurement ampoule and tested (Figure S4). Both approaches, however, failed to produce stable baselines. Thus, all successful ITC experiments to retrieve thermodynamics of adsorption were performed with one 18 carat gold agitator set to a maximum of 110 rpm allowing best possible mixing. Additionally, a low dosage speed of the injections (0.05 μL $s^{-1}$) was chosen to avoid localized high concentrations of free ligands within the suspension as encountered in Figure 2b.

### 3.3 | Adsorption Thermodynamics of Citric and Salicylic Acid on Goethite

All successful experiments showed that salicylic acid and citric acid adsorption to goethite at pH 5.5 resulted from enthalpy-driven processes that were accompanied by a loss of entropy ($\Delta H$, $\Delta S < 0$; Table 1). The stoichiometry parameter $n$ and therefore sorption capacity derived from the ITC experiment was 1.7–2.8 μmol $m^{-2}$ for citric acid adsorbed to goethite with SSA from 93 to 120 $m^2 g^{-1}$ (Table 1).

This is in close agreement with previous work on orthophosphate (not citric acid) adsorption of 2–3 μmol $m^{-2}$ to a variety of goethite samples (Strauss et al. 1997). Hence, the comparison supports the validity of our ITC results for sorption capacities. Additionally, citric acid experiments conducted with Goe-93, Goe-112, and Goe-120 (Figure 3) demonstrated that the sorption capacity on a μmol $m^{-2}$ basis of Goe-120 was 162% of the sorption capacity of Goe-93 (Table 1, stoichiometry parameter $n$) although its SSA equaled only 121% of the Goe-93 SSA. This disproportionally large increase in sorption capacity with increasing SSA points to the relevance of the abundance of defects within the crystal lattices for adsorption of citrate. Vice versa, the disproportionally large decrease in sorption capacity with decreasing SSA might also indicate that not all pore surfaces of increasingly larger mineral particles that are measured by $N_2$ adsorption are accessible for dissolved citric acid in the short time interval of the ITC experiment. This would lead to an increased time delay between injection of sorbate and adsorption to unoccupied binding sites. As a consequence, heat from diffusion-delayed adsorption may be either detected as part of the baseline drift and subtracted, or attributed to a later titration event.

The $\Delta H$ of citrate sorption to goethite ranged from 23.5 to 27.0 kJ $mol^{-1}$ (Table 1), which is similar to the $\Delta H$ value of −24.4 kJ $mol^{-1}$ for the sorption of ortho-P (2 mM solution) to gibbsite at pH 4.2 (Hong et al. 2020). The similarity of reaction enthalpies is likely due to the fact that adsorption of both, citrate and ortho-P to both goethite and gibbsite is dominated by ligand exchanges with hydroxyl surface groups of the minerals. The $\Delta G$ values we derived for the sorption of citrate to the three goethites (−18.0 to −21.0 kJ $mol^{-1}$) were slightly smaller than the value of −25.7 kJ $mol^{-1}$ reported for the sorption of ortho-P to gibbsite (Hong et al. 2020).

Both $\Delta H$ of sorption and system $\Delta S$ became more negative with increasing goethite SSA and FWHM of the 110 diffraction peak (Table 1). This trend can be explained by the increasing number of available binding sites for citric acid on goethite with lower crystallite size and greater abundance of crystal lattice defects. More binding sites enable more adsorption of molecules from aqueous solutions to mineral surfaces and thus more negative $\Delta H$. More adsorption also leads to a greater loss of $\Delta S$ due to the transition of molecules from free diffusion in solution to a more ordered state on surfaces. Hydroxyl ion-release by the ligand-exchange reaction and diffusion in solution partly counteracts the system's loss of entropy. Nevertheless, overall $\Delta S$ remains negative in all experiments since the entropy loss associated with the adsorption of dissolved organic acids due to restricted configurational freedom outweighs the entropy gained by water or hydroxyl release.

In addition, carboxyl-group oxygen atoms can bind to lattice Fe in different coordination modes. These include monodentate surface complexes, bidentate chelation to a single Fe center, and monodentate bridging between two Fe atoms. Each binding mode imposes a distinct degree of conformational freedom on the sorbed ligands: Monodentate-bound acids retain greater rotational and torsional flexibility, which leads to a smaller entropy loss compared to more constrained bidentate chelation or monodentate bridging. The more negative $\Delta S$ and smaller $\Delta G$ of citrate sorption to goethite with SSA (Goe-120 > Goe-112 > Goe-93) thus indicates that higher SSA and $FWHM_{110}$ are related to more lattice defects (Hou et al. 2022) that induce more bidentate chelation and monodentate bridging.

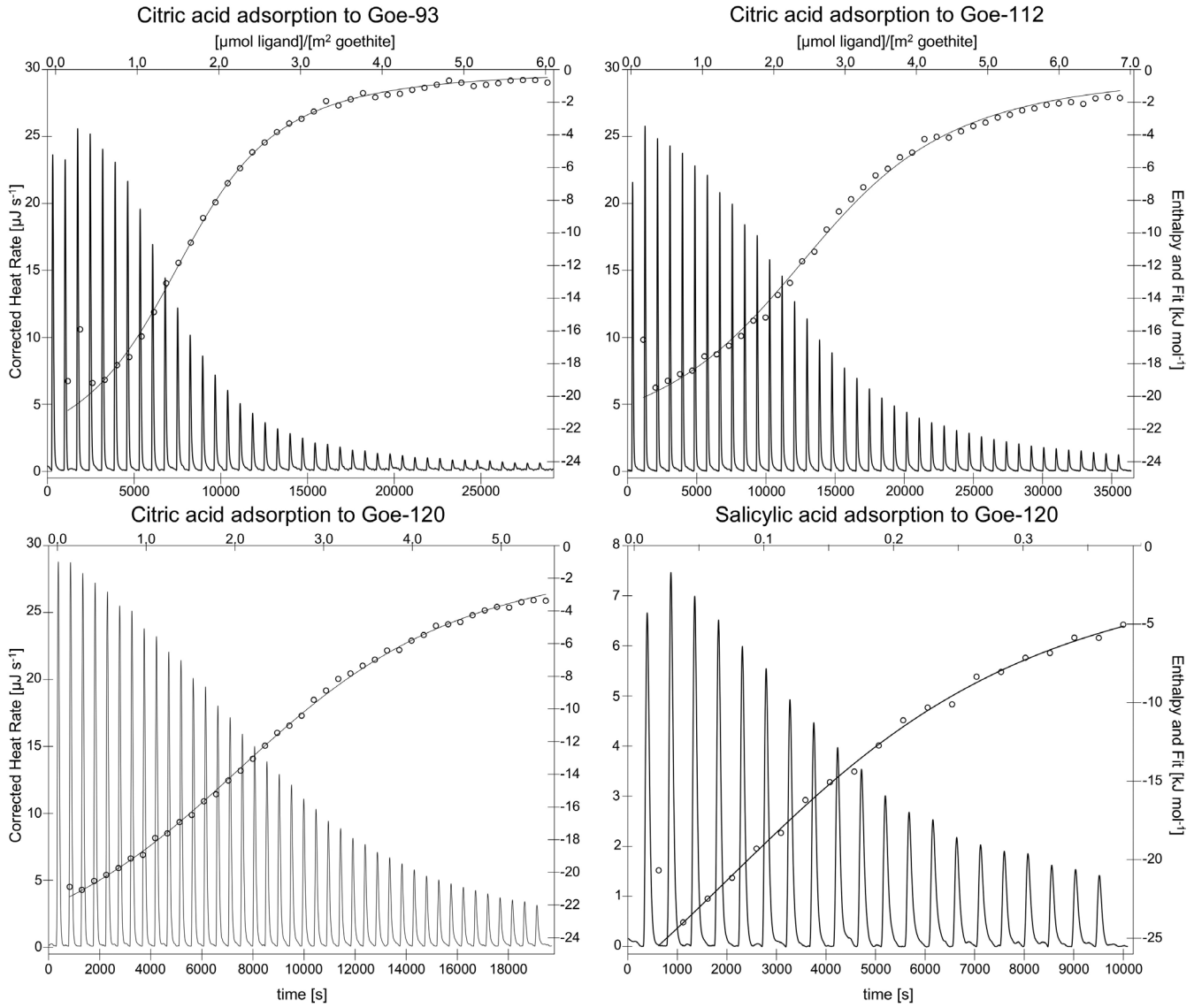


**FIGURE 3** | Thermograms and fitted independent binding models from titration experiments with citric acid and goethite minerals with specific surface areas (SSA) of 92.55 (Goe-93), 111.89 (Goe-112), and 119.56 $m^2g^{-1}$ (Goe-120), as well as salicylic acid adsorption onto goethite with SSA of 119.56 $m^2g^{-1}$after blank correction.

In comparison to citric acid, the adsorption thermodynamics of salicylic acid to goethite could only be determined for Goe-120 (Figure 3, Table 1). Surprisingly, adsorption of salicylic acid was more exothermic than that of citric acid. This cannot be explained by ligand-binding of the one carboxyl-group of salicylate to Fe on mineral surfaces. Instead, the hydroxyl group in ortho-position to the carboxyl group likely facilitated bidentate chelation with surface Fe atoms, thus leading to stronger covalent interactions and more negative $\Delta H$. Zeltner et al. (1987) as well as Yost et al. (1990) assumed a chelate structure forming between goethite and salicylic acid after investigation of FTIR spectra. Further studies of the adsorption of polyvinylalcohol to goethite (Kavanagh et al. 1976) and alcohols to hematite via chemisorption of hydroxy groups (Yun et al. 2018) support this theory. The formation of a chelate structure of salicylate with its rigid aromatic ring and possible intramolecular hydrogen bonding with the hydroxyl groups of the goethite surface would also explain the much larger loss of entropy compared to adsorption of citric acid (Table 1). Citric acid has a flexible aliphatic backbone, and thus when one or more carboxyl-groups are coordinated to surface-Fe atoms, the molecule retains rotational and torsional freedom to a higher degree compared to salicylate.

### 3.4 | Potentials, Limitations and Outlook of Isothermal Titration Calorimetry for Determining the Thermodynamics of Organo-Mineral Interactions

Virtually any molecular interaction is detectable by ITC by measuring a universal feature of such processes, namely the production or consumption of heat. However, this universality also poses a challenge to determine the thermodynamics of single processes, as heat signals from unrelated processes can interfere and complicate the measurement and deconvolution of interaction-specific heat signals (Bastos et al. 2023). Not only flocculation, which has been described within this study and in literature (Jódar-Reyes et al. 2001), but also organic acid-induced mineral dissolution

and re-crystallization (Reichard et al. 2007; Zhang et al. 1985) may lead to changes in thermograms that are not related to adsorption processes. Possible interfering processes require careful optimization and specific adjustment of experimental conditions as indicated by flocculation in our pre- and main experiments. Therefore ITC is not suitable as a high-throughput method for investigating large numbers of molecule-mineral combinations. Yet it is suitable to determine thermodynamic parameters for sorption processes with high binding affinities such as phosphate to soil colloids (Hong et al. 2020, 2021) and carboxylic acids to goethite in this study. Future developments such as the use of specialized agitators and measurement cells specifically designed for suspensions could help to minimize flocculation during ITC experiments, thereby improving experimental results and data interpretation. Furthermore, ITC could also be applied to quantify desorption processes, for example by measuring the displacement of phosphate from minerals with organic acids using phosphate-loaded minerals.

Originally, models to infer thermodynamics of binding interactions from ITC data were developed for macromolecule interactions with ligands (e.g., Claveria-Gimeno et al. 2017), not binding interactions of ligands with colloidal systems. The general assumption of simple one-site (and one reaction) binding models—including Wiseman et al. 1989 and this study—that all binding sites have the same binding affinity therefore would be violated when different binding sites of goethite crystallites (Kaiser and Guggenberger 2003, 2007; Mikutta et al. 2004; Georgieva et al. 2020) contribute similarly to the overall sorption, or if the organic acids undergo multiple sorption reactions. Several arguments nonetheless justify the application of a one-site binding model. Fourier Transform Infrared (FTIR) spectroscopic investigations of the sorption of organic acids to minerals have identified ligand exchange reaction as the dominating sorption process (Yeasmin et al. 2014; Yu et al. 2019). Molecular modeling of the sorption of the herbicide 4-Chloro-2-methylphenoxyacetic Acid (MCPA) to goethite revealed that the formation of a monodentate inner-sphere complex of the protonated MCPA species dominated the overall sorption (Kersten et al. 2014).

That a one-site and one reaction binding model well describes our ITC data supports the assumption that one sorption reaction to one type of binding site dominated the thermodynamics of sorption in our systems. The good fit of the one-site binding model also does not justify the application of a more complex model with a larger number of sorption sites, reactions and parameters, since the ITC data would not allow the unambiguous identification of parameters for additional sorption processes and binding sites. Therefore, the application of the one-site binding model to ITC measurements of sorption reactions provides useful mean values of thermodynamic sorption parameters, but the assignment of these values to individual sorption reactions and sites remains a challenge. The integration of ITC measurements at different boundary conditions like pH and ionic strength with molecular modeling of individual sorption processes could help elucidate the thermodynamics of specific sorption reactions. Such integration was, however, beyond the scope of this study.

Overall, our study demonstrates that $\Delta H$, $\Delta S$, and $\Delta G$ of sorption of low molecular weight organic acids to goethite, together with the sorption capacity for the given molecule can be determined by ITC. Moreover, variations in specific surface area, defects of the mineral lattice and sorbate configuration determine $\Delta G$ of adsorption not only via shifts in $\Delta H$, but also via modulations of $\Delta S$. Yet the consequences of sorption thermodynamics for OC persistence in soil requires $\Delta G$ values for the adsorption of a larger range of organic compounds to different minerals in combination with incubation experiments with isotope-labeled organic compounds.

In an initial application of this approach, we found that up to 71% of citric acid adsorbed to goethite (Goe-93 in this study) was inaccessible to microbes when incubated in arable topsoil, while only 36% of goethite-adsorbed salicylic acid remained inaccessible (Konrad et al. 2025). This suggests that the $\Delta G$ of sorption of approximately $-21\,\mathrm{kJ\,mol^{-1}}$ does not represent an energetic barrier in soil systems that completely prevents the biological processing of citrate and salicylate sorbed to goethite. Furthermore, position-specific labeled carboxyl-C from phenylalanine and salicylic acid coordinated to goethite showed an even higher bio-accessibility (up to 82% of all adsorbed C) and faster mineralization compared to the overall molecule (Konrad et al. 2026). Thus, adsorption via ligand-binding per se does not prevent microbial processing.

## 4 | Conclusions

By quantifying the thermodynamics of adsorption of citric acid and salicylic acid to goethite, we show that higher SSA and lattice defects strengthen binding and constrain ligand conformation. Although ITC is sensitive to flocculation, its direct heat measurements provide unique thermodynamic insight into the binding of organic ligands to minerals. These insights could improve prediction of soil organic carbon persistence and information on soil carbon cycling. Future work should broaden the ligand- and mineral suite, examine pH effects, develop instrumentation to mitigate flocculation, and integrate ITC measurements with molecular modeling of sorption processes to improve the assignment of thermodymamic data to individual sorption reactions.

### Author Contributions

**Alexander Konrad:** investigation, writing – original draft, writing – review and editing, visualization, validation, methodology, software, formal analysis, data curation. **Ines Mulder:** conceptualization, data curation, project administration. **Diana Hofmann:** writing – review and editing, validation, supervision, methodology. **Friederike Lang:** conceptualization, funding acquisition, validation, writing – review and editing. **Kenton P. Stutz:** conceptualization, supervision, writing – review and editing, funding acquisition. **Jan Siemens:** conceptualization, methodology, investigation, validation, funding acquisition, supervision, writing – review and editing, data curation, resources, project administration.

### Acknowledgments

This work was funded by the German Research Foundation (DFG, grant no. 465123895). Experimental data were obtained within the DFG Priority Program 2322 "Systems ecology of soils—Energy Discharge Modulated by Microbiome and Boundary Conditions (SoilSystems)". We thank the staff of the core projects, the Priority Program office and the BExIS team for their work in maintaining the project infrastructure, and the Priority Program Scientific Committee for their role in setting up the project. We gratefully honor the memory of Gerhard Brümmer,

to whom we owe the Goe-120. We thank Kai Jansen for preparing and providing the goethite with the SSA of 93 $m^2 g^{-1}$. We would like to thank Martin Kaupenjohann for his idea and foresight to employ isothermal titration calorimetry to obtain the thermodynamics of adsorption processes on soil minerals and for the possibility of using the calorimeter. Furthermore, we express our gratitude to Anne Wagner, Maike Mai and Jaane Krüger for their invaluable help in setting up the calorimeter, as well as Ralf Sack, precision mechanics workshop JLU Giessen, for helping out with fixing calorimeter shafts and agitators when these delicate parts could not handle soil science.

### Funding

This work was supported by Deutsche Forschungsgemeinschaft.

### Conflicts of Interest

The authors declare no conflicts of interest.

### Data Availability Statement

The data that support the findings of this study are available on request from the corresponding author. The data are not publicly available due to privacy or ethical restrictions.

### References

Bastos, M., O. Abian, C. M. Johnson, et al. 2023. "Isothermal Titration Calorimetry." *Nature Reviews Methods Primers* 3, no. 1: 17. https://doi.org/10.1038/s43586-023-00199-x.

Blakey, B. C., and D. F. James. 2003. "The Viscous Behaviour and Structure of Aqueous Suspensions of Goethite." *Colloids and Surfaces A: Physicochemical and Engineering Aspects* 231, no. 1–3: 19–30. https://doi.org/10.1016/j.colsurfa.2003.08.019.

Bramble, D. S. E., S. Ulrich, I. Schöning, et al. 2024. "Formation of Mineral-Associated Organic Matter in Temperate Soils Is Primarily Controlled by Mineral Type and Modified by Land Use and Management Intensity." *Global Change Biology* 30, no. 1: e17024. https://doi.org/10.1111/gcb.17024.

Claveria-Gimeno, R., P. M. Lanuza, I. Morales-Chueca, et al. 2017. "The Intervening Domain from MeCP2 enhances the DNA Affinity of The Methyl Binding Domain and Provides an Independent DNA Interaction Site." *Scientific Reports* 7, no. 1: 41635. https://doi.org/10.1038/srep41635.

Cornell, R. M., and U. Schwertmann. 2003. *The Iron Oxides: Structure, Properties, Reactions, Occurrences and Uses*. 2nd ed. Wiley-VCH.

Dultz, S., S. K. Woche, R. Mikutta, M. Schrapel, and G. Guggenberger. 2019. "Size and Charge Constraints in Microaggregation: Model Experiments With Mineral Particle Size Fractions." *Applied Clay Science* 170: 29–40. https://doi.org/10.1016/j.clay.2019.01.002.

Echigo, T., T. Hatta, S. Nemoto, and S. Takizawa. 2012. "X-Ray Photoelectron Spectroscopic Study on the Goethites With Variations in Crystallinity and Morphology: Their Effects on Surface Hydroxyl Concentration." *Physics and Chemistry of Minerals* 39, no. 9: 769–778. https://doi.org/10.1007/s00269-012-0531-y.

Eilers, P. H. C., and H. F. M. Boelens. 2005. *Baseline Correction With Asymmetric Least Squares Smoothing*. Vol. 1, 5. Leiden University Medical Centre Report.

Feng, W., A. F. Plante, and J. Six. 2013. "Improving Estimates of Maximal Organic Carbon Stabilization by Fine Soil Particles." *Biogeochemistry* 112, no. 1–3: 81–93. https://doi.org/10.1007/s10533-011-9679-7.

Fischer, L., G. W. Brümmer, and N. J. Barrow. 1998. "Zur Kinetik der Sorption von Schwermetallen an Bodenkomponenten. I. Sorptions- und Diffusionsprozesse an/in Goethitpartikeln." *Mittelstandsanleihen Deutsche Bodenkundliche Gesellschaft* 88: 171–174.

Freire, E., O. L. Mayorga, and M. Straume. 1990. "Isothermal Titration Calorimetry." *Analytical Chemistry* 62, no. 18: 950A–959A. https://doi.org/10.1021/ac00217a002.

Gao, J., B. Jansen, C. Cerli, et al. 2018. "Organic Matter Coatings of Soil Minerals Affect Adsorptive Interactions With Phenolic and Amino Acids." *European Journal of Soil Science* 69, no. 4: 613–624. https://doi.org/10.1111/ejss.12562.

Georgieva, I., M. Kersten, and D. Tunega. 2020. "Molecular Modeling of MCPA Herbicide Adsorption by Goethite (110) Surface in Dependence of pH." *Theoretical Chemistry Accounts* 139, no. 8: 132. https://doi.org/10.1007/s00214-020-02646-4.

Georgiou, K., R. B. Jackson, O. Vindušková, et al. 2022. "Global Stocks and Capacity of Mineral-Associated Soil Organic Carbon." *Nature Communications* 13, no. 1: 3797. https://doi.org/10.1038/s41467-022-31540-9.

Goodman, B. A., and D. G. Lewis. 1981. "Mössbauer Spectra of Aluminous Goethites (α-FeOOH)." *Journal of Soil Science* 32, no. 3: 351–364. https://doi.org/10.1111/j.1365-2389.1981.tb01711.x.

Guo, H., and A. S. Barnard. 2013. "Naturally Occurring Iron Oxide Nanoparticles: Morphology, Surface Chemistry and Environmental Stability." *Journal of Materials Chemistry A* 1, no. 1: 27–42. https://doi.org/10.1039/C2TA00523A.

Hong, Z., J. Yan, J. Jiang, J. Li, and R. Xu. 2021. "Direct Quantification of Sorption Thermodynamics of Phosphate on Four Soil Colloids Through Isothermal Titration Calorimetry." *ACS Earth and Space Chemistry* 5, no. 2: 295–304. https://doi.org/10.1021/acsearthspacechem.0c00281.

Hong, Z.-n., J. Yan, J. Jiang, J. Li, and R. Xu. 2020. "Isothermal Titration Calorimetry as a Useful Tool to Examine Adsorption Mechanisms of Phosphate on Gibbsite at Various Solution Conditions." *Soil Science Society of America Journal* 84, no. 4: 1110–1124. https://doi.org/10.1002/saj2.20101.

Hou, J., X. Tan, Y. Xiang, et al. 2022. "Insights Into the Underlying Effect of Fe Vacancy Defects on the Adsorption Affinity of Goethite for Arsenic Immobilization." *Environmental Pollution* 314: 120268. https://doi.org/10.1016/j.envpol.2022.120268.

Jódar-Reyes, A. B., A. Martín-Rodríguez, and J. L. Ortega-Vinuesa. 2001. "An Enthalpic Analysis on the Aggregation of Colloidal Particles Studied by Microcalorimetry." *Journal of Colloid and Interface Science* 237, no. 1: 6–10. https://doi.org/10.1006/jcis.2001.7429.

Jones, D. L., and A. C. Edwards. 1998. "Influence of Sorption on the Biological Utilization of Two Simple Carbon Substrates." *Soil Biology & Biochemistry* 30, no. 14: 1895–1902. https://doi.org/10.1016/S0038-0717(98)00060-1.

Joshi, H., P. S. Shirude, V. Bansal, K. N. Ganesh, and M. Sastry. 2004. "Isothermal Titration Calorimetry Studies on the Binding of Amino Acids to Gold Nanoparticles." *Journal of Physical Chemistry B* 108, no. 31: 11535–11540. https://doi.org/10.1021/jp048766z.

Kaiser, K., and G. Guggenberger. 2003. "Mineral Surfaces and Soil Organic Matter." *European Journal of Soil Science* 54, no. 2: 219–236. https://doi.org/10.1046/j.1365-2389.2003.00544.x.

Kaiser, K., and G. Guggenberger. 2007. "Sorptive Stabilization of Organic Matter by Microporous Goethite: Sorption Into Small Pores vs. Surface Complexation." *European Journal of Soil Science* 58, no. 1: 45–59. https://doi.org/10.1111/j.1365-2389.2006.00799.x.

Kavanagh, B. V., A. M. Posner, and J. P. Quirk. 1976. "The Adsorption of Polyvinyl Alcohol on Gibbsite and Goethite." *Journal of Soil Science* 27, no. 4: 467–477. https://doi.org/10.1111/j.1365-2389.1976.tb02016.x.

Kersten, M., D. Tunega, I. Georgieva, N. Vlasova, and R. Branscheid. 2014. "Adsorption of the Herbicide 4-Chloro-2-Methylphenoxyacetic Acid (MCPA) by Goethite." *Environmental Science & Technology* 48, no. 20: 11803–11810. https://doi.org/10.1021/es502444c.

Konrad, A., D. Hofmann, J. Siemens, F. Lang, I. Mulder, and K. P. Stutz. 2026. "Rapid Mineralization of Mineral-Bound Carboxyl-Carbon of Salicylic Acid and Phenylalanine." *Soil Biology and Biochemistry* 212: 110016. https://doi.org/10.1016/j.soilbio.2025.110016.

Konrad, A., D. Hofmann, J. Siemens, K. P. Stutz, F. Lang, and I. Mulder. 2025. "Microbial Carbon Use Efficiency of Mineral-Associated Organic Matter Is Related to Its Desorbability." *Soil Biology and Biochemistry* 203: 109740. https://doi.org/10.1016/j.soilbio.2025.109740.

Kumar, S., R. M. R. Dumpala, A. Chandane, and J. Bahadur. 2022. "Elucidation of the Sorbent Role in Sorption Thermodynamics of Uranium(VI) on Goethite." *Environmental Science: Processes & Impacts* 24, no. 4: 567–575. https://doi.org/10.1039/D1EM00380A.

Madsen, D. E., L. Cervera-Gontard, T. Kasama, et al. 2009. "Magnetic Fluctuations in Nanosized Goethite (α-FeOOH) Grains." *Journal of Physics: Condensed Matter* 21, no. 1: 016007. https://doi.org/10.1088/0953-8984/21/1/016007.

Mikutta, C., F. Lang, and M. Kaupenjohann. 2004. "Soil Organic Matter Clogs Mineral Pores: Evidence from$^{1}$ H-NMR and $N_2$ Adsorption." *Soil Science Society of America Journal* 68, no. 6: 1853–1862. https://doi.org/10.2136/sssaj2004.1853.

Penn, C. J., and J. G. Warren. 2009. "Investigating Phosphorus Sorption Onto Kaolinite Using Isothermal Titration Calorimetry." *Soil Science Society of America Journal* 73, no. 2: 560–568. https://doi.org/10.2136/sssaj2008.0198.

Penn, C. J., and H. Zhang. 2010. "Isothermal Titration Calorimetry as an Indicator of Phosphorus Sorption Behavior." *Soil Science Society of America Journal* 74, no. 2: 502–511. https://doi.org/10.2136/sssaj2009.0199.

Prozeller, D., S. Morsbach, and K. Landfester. 2019. "Isothermal Titration Calorimetry as a Complementary Method for Investigating Nanoparticle–Protein Interactions." *Nanoscale* 11, no. 41: 19,265–19,273. https://doi.org/10.1039/C9NR05790K.

Reichard, P. U., R. Kretzschmar, and S. M. Kraemer. 2007. "Dissolution Mechanisms of Goethite in the Presence of Siderophores and Organic Acids." *Geochimica et Cosmochimica Acta* 71, no. 23: 5635–5650. https://doi.org/10.1016/j.gca.2006.12.022.

Saidy, A. R., R. J. Smernik, J. A. Baldock, K. Kaiser, and J. Sanderman. 2015. "Microbial Degradation of Organic Carbon Sorbed to Phyllosilicate Clays With and Without Hydrous Iron Oxide Coating: Mineralization of OC-Clay-Oxide Associations." *European Journal of Soil Science* 66, no. 1: 83–94. https://doi.org/10.1111/ejss.12180.

Saidy, A. R., R. J. Smernik, J. A. Baldock, K. Kaiser, J. Sanderman, and L. M. Macdonald. 2012. "Effects of Clay Mineralogy and Hydrous Iron Oxides on Labile Organic Carbon Stabilisation." *Geoderma* 173–174: 104–110. https://doi.org/10.1016/j.geoderma.2011.12.030.

Schrumpf, M., K. Kaiser, G. Guggenberger, T. Persson, I. Kögel-Knabner, and E.-D. Schulze. 2013. "Storage and Stability of Organic Carbon in Soils as Related to Depth, Occlusion Within Aggregates, and Attachment to Minerals." *Biogeosciences* 10, no. 3: 1675–1691. https://doi.org/10.5194/bg-10-1675-2013.

Schwertmann, U., P. Cambier, and E. Murad. 1985. "Properties of Goethites of Varying Crystallinity." *Clays and Clay Minerals* 33, no. 5: 369–378. https://doi.org/10.1346/CCMN.1985.0330501.

Spielvogel, S., J. Prietzel, and I. Kgel-Knabner. 2008. "Soil Organic Matter Stabilization in Acidic Forest Soils Is Preferential and Soil Type-Specific." *European Journal of Soil Science* 59, no. 4: 674–692. https://doi.org/10.1111/j.1365-2389.2008.01030.x.

Strauss, R., G. W. Brümmer, and N. J. Barrow. 1997. "Effects of Crystallinity of Goethite: II. Rates of Sorption and Desorption of Phosphate." *European Journal of Soil Science* 48, no. 1: 101–114. https://doi.org/10.1111/j.1365-2389.1997.tb00189.x.

Taitel-Goldman, N., C. Bender Koch, and A. Singer. 2004. "Si-Associated Goethite in Hydrothermal Sediments of the Atlantis II and Thetis Deeps, Red Sea." *Clays and Clay Minerals* 52, no. 1: 115–129. https://doi.org/10.1346/CCMN.2004.0520111.

Wiseman, T., S. Williston, J. F. Brandts, and L.-N. Lin. 1989. "Rapid Measurement of Binding Constants and Heats of Binding Using a New Titration Calorimeter." *Analytical Biochemistry* 179, no. 1: 131–137. https://doi.org/10.1016/0003-2697(89)90213-3.

Yeasmin, S., B. Singh, R. S. Kookana, M. Farrell, D. L. Sparks, and C. T. Johnston. 2014. "Influence of Mineral Characteristics on the Retention of Low Molecular Weight Organic Compounds: A Batch Sorption–Desorption and ATR-FTIR Study." *Journal of Colloid and Interface Science* 432: 246–257. https://doi.org/10.1016/j.jcis.2014.06.036.

Yost, E. C., M. I. Tejedor-Tejedor, and M. A. Anderson. 1990. "In Situ CIR-FTIR Characterization of Salicylate Complexes at the Goethite/Aqueous Solution Interface." *Environmental Science & Technology* 24, no. 6: 822–828. https://doi.org/10.1021/es00076a005.

Yu, C., J. Bahashi, and E. Bi. 2019. "Mechanisms and Quantification of Adsorption of Three Anti-Inflammatory Pharmaceuticals Onto Goethite With/Without Surface-Bound Organic Acids." *Chemosphere* 222: 593–602. https://doi.org/10.1016/j.chemosphere.2019.01.155.

Yun, D., C. Krutpijit, B. Jongsomjit, and J. E. Herrera. 2018. "Asymmetrical Coexistence of Associatively and Dissociatively Adsorbed Alcohol Species Over α-Fe2O3 Iron Oxide Nanoparticles." *Surface Science* 677: 203–212. https://doi.org/10.1016/j.susc.2018.07.005.

Zeltner, W. A., E. C. Yost, M. L. Machesky, M. I. Tejedor-Tejedor, and M. A. Anderson. 1987. "Characterization of Anion Binding on Goethite Using Titration Calorimetry and Cylindrical Internal Reflection-Fourier Transform Infrared Spectroscopy." In *Geochemical Processes at Mineral Surfaces*, Chapter 8, 142–161. American Chemical Society.

Zhang, Y., N. Kallay, and E. Matijevic. 1985. "Interaction of Metal Hydrous Oxides With Chelating Agents. 7. Hematite-Oxalic Acid and -Citric Acid Systems." *Langmuir* 1, no. 2: 201–206. https://doi.org/10.1021/la00062a004.

## Supporting Information

Additional supporting information can be found online in the Supporting Information section. **Figure S1:** Workflow from raw data to model development. Raw calorimetric data were first imported into OriginPro 2024b (a). Baseline shifts were corrected using the asymmetric least-squares regression function (b, c), and the processed data were exported as .txt files to NanoAnalyze. In NanoAnalyze, titration steps and experimental parameters were defined, and blank titration data were subtracted (d). The resulting, blank-corrected data served as the basis for model building (e). **Figure S2:** Thermograms and independent one-site model fits of citric acid adsorption at pH 5.5 to goethite with a surface area of 119.56 $m^2 g^{-1}$ with different inputs for the concentration of sorbent: top shows stoichiometry $n$ as binding sites goethite per $m^2$ surface area with concentration of sorbent expressed in the unit [$m^2$ mineral surface $L^{-1}$]. The bottom model uses the stoichiometry from the top shown model [μmol $m^{-2}$] multiplied by the mineral surface area per liter suspension to yield the sorbent concentration in the unit [μmol binding sites $L^{-1}$] as input. The thermodynamics derived from both models are identical, with $n$ from the first model (top) giving the sorption capacity, while the second models $n$ yields the typical, unitless 1:1 binding stoichiometry. **Figure S3:** Linear regression between specific surface area and full width at half maximum of the 110 diffraction peak ($FWHM_{110}$) of the goethite samples used for this study. **Figure S4:** Agitator modifications to overcome flocculation of mineral suspension during titration experiments. Left shows double-stacked standard agitators with shortened shafts from TA Instruments Inc. (Newcastle, Delaware, USA). Right shows 3D-printed helical polypropylene agitator.